IOP Publishing Journal of Physics A: Mathematical and Theoretical
J. Phys. A: Math. Theor. **47** (2014) 035302 (20pp) doi:10.1088/1751-8113/47/3/035302

Geometric quantum discord with Bures distance: the qubit case

D Spehner[1,2] **and M Orszag**[3]

[1] Université Grenoble 1 and CNRS, Institut Fourier UMR5582, B.P. 74, F-38402 Saint Martin d'Hères, France
[2] Université Grenoble 1 and CNRS, Laboratoire de Physique et Modélisation des Milieux Condensés UMR5493, B.P. 166, F-38042 Grenoble, France
[3] Pontificia Universidad Católica, Facultad de física, Casilla 306, Santiago 22, Chile

E-mail: Dominique.Spehner@ujf-grenoble.fr

Received 28 August 2013, revised 3 September 2013
Accepted for publication 20 November 2013
Published 20 December 2013

Abstract

The minimal Bures distance of a quantum state of a bipartite system AB to the set of classical states for subsystem A defines a geometric measure of quantum discord. When A is a qubit, we show that this geometric quantum discord is given in terms of the eigenvalues of a $(2n_B) \times (2n_B)$ Hermitian matrix, n_B being the Hilbert space dimension of the other subsystem B. As a first application, we calculate the geometric discord for the output state of the DQC1 algorithm. We find that it takes its highest value when the unitary matrix from which the algorithm computes the trace has its eigenvalues uniformly distributed on the unit circle modulo a symmetry with respect to the origin. As a second application, we derive an explicit formula for the geometric discord of a two-qubit state ρ with maximally mixed marginals and compare it with other measures of quantum correlations. We also determine the closest classical states to ρ.

PACS numbers: 03.67.Mn, 03.67.Hk

(Some figures may appear in colour only in the online journal)

1. Introduction

In order to understand the origin of quantum speedups in quantum algorithms and to analyze the specificities of quantum communication protocols, it is of prime importance to identify the resources needed to have a quantum advantage [1]. Despite substantial progress in the last decades [2, 3], a complete characterization of quantum correlations (QCs) in composite quantum systems has not yet emerged, even for bipartite systems. Furthermore, the role

played by these correlations in information processing tasks remains to a large extent unclear. The quantum discord (QD) is one measure of QCs in bipartite systems [4, 5]. It coincides with the entanglement of formation [6] for pure states, but for mixed states it quantifies QCs that may be present even in separable states. The discord is believed to be a better indicator than entanglement of the 'degree of quantumness' of mixed states. Moreover, it has been suggested [7–10] that it could capture the relevant quantum resource in Knill and Laflamme's algorithm of deterministic quantum computation with one qubit (DQC1) [11]. This algorithm allows to compute efficiently the trace of a $2^n \times 2^n$ unitary matrix U_n. It involves a polarized control qubit, which remains unentangled with n unpolarized target qubits at all stages of the computation. The amount of entanglement for any bipartition of the $(n+1)$ qubits is bounded independently of n [12]. However, a non-vanishing QD between the control and the n target qubits appears in the output state [7–10], save for some particular unitaries U_n [8, 13].

In a recent article [14], we have proposed to use the Bures distance to the set of zero-discord states as a geometrical analogue of the QD. This geometric QD (GQD) does not suffer the drawbacks of a similar measure introduced by Dakić *et al* [13], which makes use of the Hilbert–Schmidt distance. In particular, for pure states the Bures-GQD is equal to the geometric measure of entanglement defined as the Bures distance to the set of separable states [15, 16]. The main advantage of the geometric approach is that, in addition to quantifying the degree of quantumness of a given state ρ, one can look for the closest zero-discord states to ρ. This may help to understand decoherence processes and peculiar features of QCs during dynamical evolutions, such as the sudden transitions discussed in [17, 18]. The main result of [14] is that the Bures-GQD of a mixed state ρ is equal to the maximal success probability in ambiguous quantum state discrimination (QSD) of a family of states ρ_i depending on ρ. Moreover, the closest zero-discord states to ρ are given in terms of the optimal von Neumann measurement in this discrimination task.

In this paper, we apply the aforementioned results [14] in order to calculate the Bures-GQD when one subsystem of the bipartite system is a qubit. In particular, we determine the GQD between the control qubit and the n target qubits of the output state in the DQC1 algorithm. We show that for any unitary matrix U_n, the discord is bounded from above by its value obtained by choosing random unitaries distributed according to the Haar measure. We also derive an explicit formula for states ρ of two qubits with maximally mixed marginals and determine the closest zero-discord states to ρ. We compare our results to those obtained by using the Hilbert–Schmidt distance and the relative entropy.

The layout of the paper is as follows. We recall in section 2 the problem of ambiguous QSD, the definitions of the QDs, and the link between the geometric discord and QSD. In section 3, we show how to solve the QSD task and determine the GQD when the measured subsystem is a qubit. We calculate in section 4 the GQD for the output state in the DQC1 model. Section 5 is devoted to the case of two qubits. We compare our results for the GQD with the other QDs and find the closest zero-discord states to a Bell-diagonal state. The last section 6 contains conclusive remarks. Some technical details are presented in the appendix.

2. Quantum state discrimination and the geometric quantum discord

2.1. Ambiguous quantum state discrimination

The objective of QSD consists in distinguishing states taken randomly from a known ensemble of states [19, 20]. If these states are non-orthogonal, any measurement devised to distinguish them cannot succeed to identify exactly which state from the ensemble has been chosen. The QSD task is to find the optimal measurements leading to the smallest probability of

equivocation. More precisely, a receiver is given a state ρ_i in a finite dimensional Hilbert space $\mathcal{H}$, drawn from a known family $\{\rho_i\}_{i=1}^{n_A}$, with a prior probability η_i. In order to determine which state he has received, he performs a generalized measurement and concludes that the state is ρ_j when he gets the measurement outcome j. The probability to find this outcome given that the state is ρ_i is $P_{j|i} = \mathrm{tr}(M_j\rho_i)$, where $\{M_j\}$ is a family of non-negative measurement operators satisfying $\sum_j M_j = 1$ (POVM). In the so-called ambiguous QSD strategy, the number of measurement outcomes is chosen to be equal to the number n_A of states in the ensemble $\{\rho_i, \eta_i\}$. The maximal success probability of the receiver reads

$$P_S^{\mathrm{opt}}(\{\rho_i, \eta_i\}) = \max_{\mathrm{POVM}\ \{M_i\}} \sum_{i=1}^{n_A} \eta_i \,\mathrm{tr}(M_i\rho_i). \tag{1}$$

If the ρ_i have rank $n_B = \dim(\mathcal{H})/n_A$ and are linearly independent, in the sense that their eigenvectors $|\xi_{ij}\rangle$ with nonzero eigenvalues form a linearly independent family $\{|\xi_{ij}\rangle\}_{i=1,\ldots,n_A}^{j=1,\ldots,n_B}$ of vectors in $\mathcal{H}$, it is known [21] that the optimal POVM $\{M_i^{\mathrm{opt}}\}_{i=1}^{n_A}$ is a von Neumann measurement with projectors of rank n_B. Therefore, in that case $P_S^{\mathrm{opt}}(\{\rho_i, \eta_i\}) = P_S^{\mathrm{opt\,v.N.}}(\{\rho_i, \eta_i\})$, where

$$P_S^{\mathrm{opt\,v.N.}}(\{\rho_i, \eta_i\}) = \max_{\{\Pi_i\}} \sum_{i=1}^{n_A} \eta_i \,\mathrm{tr}(\Pi_i\rho_i) \tag{2}$$

is the maximum success probability over all orthogonal families $\{\Pi_i\}_{i=1}^{n_A}$ of projectors of rank n_B (i.e., self-adjoint operators satisfying $\Pi_i\Pi_j = \delta_{ij}\Pi_i$ and $\mathrm{rank}(\Pi_i) = n_B$).

2.2. Quantum discords

We first briefly recall the definition of the QD of Ollivier and Zurek and Henderson and Vedral [4, 5]. Let AB be a bipartite system in the state ρ. The mutual information of AB is given by $I_{A:B}(\rho) = S(\rho_A) + S(\rho_B) - S(\rho)$, where $S(\cdot)$ stands for the von Neumann entropy and $\rho_A = \mathrm{tr}_B(\rho)$ and $\rho_B = \mathrm{tr}_A(\rho)$ are the reduced states of A and B, respectively. The mutual information is non-negative by the sub-additivity of S. It characterizes the total (classical and quantum) correlations in AB. The QD measures the amount of mutual information which is not accessible by local measurements on the subsystem A. It can be defined as

$$\delta_A(\rho) = I_{A:B}(\rho) - \max_{\{\pi_i^A\}} I_{A:B}(\mathcal{M}_{\{\pi_i^A\}}(\rho)), \tag{3}$$

where the maximum is over all von Neumann measurements (i.e., orthogonal families of projectors) $\{\pi_i^A\}$ on A and $\mathcal{M}_{\{\pi_i^A\}}(\rho) = \sum_i \pi_i^A \otimes 1\, \rho\, \pi_i^A \otimes 1$ is the post-measurement state in the absence of readout. The second term in (3) represents the amount of classical correlations. It can be shown that $\delta(\rho) \geqslant 0$ and $\delta_A(\sigma_{A-\mathrm{cl}}) = 0$ if and only if

$$\sigma_{A\text{-cl}} = \sum_{i=1}^{n_A} q_i |\alpha_i\rangle\langle\alpha_i| \otimes \sigma_{B|i}, \tag{4}$$

where $\{|\alpha_i\rangle\}_{i=1}^{n_A}$ is an orthonormal basis for subsystem A, $\sigma_{B|i}$ are some (arbitrary) states of B depending on the index i, and $q_i \geqslant 0$ are some probabilities. We call A-classical states the zero-discord states of the form (4). [4]

The set of quantum states can be equipped with various distances. From a quantum information perspective, it is natural to study the geometry induced by the Bures distance [1, 22, 23]

$$d_B(\rho, \sigma) = \left[2\left(1 - \sqrt{F(\rho, \sigma)}\right)\right]^{\frac{1}{2}}, \tag{5}$$

[4] In the literature these states are often referred to as the 'classical-quantum' states.

where $F(\rho,\sigma)$ is the Uhlmann fidelity

$$F(\rho,\sigma)=\left\|\sqrt{\rho}\sqrt{\sigma}\right\|_1^2=\left[\mathrm{tr}\left(\left[\sqrt{\sigma}\rho\sqrt{\sigma}\right]^{1/2}\right)\right]^2 \tag{6}$$

generalizing the usual pure-state fidelity $|\langle\Psi|\Phi\rangle|^2$. The distance d_B pertains to the family of monotonous (that is, contractive with respect to completely positive trace-preserving maps) Riemannian distances [24]. Its metric coincides with the quantum Fisher information playing an important role in quantum metrology [25]. We take this opportunity to mention a misprint in our previous article [14]: although the square distance $d_B(\rho,\sigma)^2$ is jointly convex, this is not the case for $d_B(\rho,\sigma)$.

The GQD is by definition the square distance of ρ to the set $\mathcal{C}_A$ of A-classical states,

$$D_A(\rho)=d_B(\rho,\mathcal{C}_A)^2\equiv\min_{\sigma_{A\text{-cl}}\in\mathcal{C}_A}d_B(\rho,\sigma_{A\text{-cl}})^2. \tag{7}$$

One can similarly define the discord $D_B(\rho)=d_B(\rho,\mathcal{C}_B)^2$, where $\mathcal{C}_B$ is the set of B-classical states. One has in general $D_B\neq D_A$ (in fact, it is clear from the form (4) of the A-classical states that $\mathcal{C}_B\neq\mathcal{C}_A$). The same holds for the discords $\delta_A\neq\delta_B$, because the maximal mutual informations after measuring subsystems A or B are in general different. It is not difficult to show [14] that for pure states D_A and D_B coincide with the geometric measure of entanglement $E(\rho)=\min_{\sigma_{\mathrm{sep}}\in\mathcal{S}}d_B(\rho,\sigma_{\mathrm{sep}})^2$, where $\mathcal{S}$ denotes the convex set of separable states. More precisely, if $\rho_\Psi=|\Psi\rangle\langle\Psi|$ then $D_A(\rho_\Psi)=D_B(\rho_\Psi)=E(\rho_\Psi)=2(1-\sqrt{\mu_{\max}})$, $\mu_{\max}$ being the highest eigenvalue of $(\rho_\Psi)_A$ (maximal Schmidt coefficient). This equality between D_A, D_B, and E comes from the fact that the closest separable state to a pure state is a pure product state[5].

2.3. Link between D_A and state discrimination

The evaluation of the GQD (7) for mixed states ρ turns out to be related to an ambiguous QSD task [14]. More precisely, the fidelity between ρ and its closest A-classical state is given by the maximum success probability (2),

$$F_A(\rho)\equiv\max_{\sigma_{A\text{-cl}}\in\mathcal{C}_A}F(\rho,\sigma_{A\text{-cl}})=\max_{\{|\alpha_i\rangle\}}P_S^{\text{opt v.N.}}(\{\rho_i,\eta_i\}). \tag{8}$$

In the right-hand side, the maximum is over all orthonormal basis $\{|\alpha_i\rangle\}_{i=1}^{n_A}$ of A and $\{\rho_i,\eta_i\}_{i=1}^{n_A}$ is an ensemble of states depending on $\{|\alpha_i\rangle\}$ and ρ defined by

$$\eta_i=\langle\alpha_i|\rho_A|\alpha_i\rangle,\qquad\rho_i=\eta_i^{-1}\sqrt{\rho}|\alpha_i\rangle\langle\alpha_i|\otimes 1\sqrt{\rho} \tag{9}$$

(if $\eta_i=0$ then ρ_i is not defined but does not contribute to the success probability). The number of states ρ_i is equal to the dimension n_A of the Hilbert space of A. It is easy to see that if $\rho>0$ then all the ρ_i have ranks equal to the dimension n_B of the space of B. Furthermore, they are linearly independent. Thus $P_S^{\text{opt v.N.}}$ can be replaced by P_S^{opt} in equation (8).

Note that $\{\rho_i,\eta_i\}$ defines a convex decomposition of ρ, $\rho=\sum_i\eta_i\rho_i$. A remarkable property of this decomposition is that the associated square-root measurement operators $M_i=\eta_i\rho^{-1/2}\rho_i\rho^{-1/2}$, which are known to be optimum in the ambiguous QSD of symmetric ensembles [26, 27], coincide with the projectors $\Pi_i=|\alpha_i\rangle\langle\alpha_i|\otimes 1$. By bounding from below $P_S^{\text{opt v.N.}}(\{\rho_i,\eta_i\})$ by the success probability corresponding to Π_i, we obtain

$$F_A(\rho)\geqslant\max_{\{|\alpha_i\rangle\}}\sum_{i=1}^{n_A}\mathrm{tr}_B\left[\langle\alpha_i|\sqrt{\rho}|\alpha_i\rangle^2\right]. \tag{10}$$

[5] More precisely, a pure state can have either a unique closest separable state given by a pure product state or, if the maximal Schmidt coefficient $\mu_{\max}$ is degenerate, infinitely many closest separable states, given by convex combinations of orthogonal pure product states (see [14]).

Let us denote by $\{|\alpha_i^{\rm opt}\rangle\}$ and $\{\Pi_i^{\rm opt}\}$ the basis and projective measurement(s) maximizing $P_S^{\text{opt v.N.}}(\{\rho_i, \eta_i\})$ in (8). Then the closest A-classical state(s) to ρ is (are) [14]

$$\sigma_\rho = \frac{1}{F_A(\rho)} \sum_{i=1}^{n_A} |\alpha_i^{\rm opt}\rangle\langle\alpha_i^{\rm opt}| \otimes \langle\alpha_i^{\rm opt}|\sqrt{\rho}\,\Pi_i^{\rm opt}\sqrt{\rho}|\alpha_i^{\rm opt}\rangle. \tag{11}$$

Finding analytically the optimal success probability and optimal measurement(s) in ambiguous QSD with $n_A > 2$ states is an open problem, excepted for symmetric ensembles [20, 26, 27]. A necessary and sufficient condition for a POVM to be optimum is due to Helstrom [19]. Various bounds on $P_S^{\rm opt}$ have been derived in the literature (see [28] and references therein). Moreover, efficient methods are available to solve this problem numerically [29, 30]. We focus in the next section on the simpler case $n_A = 2$, for which an analytic solution is well-known.

3. Geometric discord for a $(2, n_B)$ bipartite system

If the subsystem A is a qubit, the ensemble $\{\rho_i, \eta_i\}$ contains only $n_A = 2$ states and the QSD task can be easily handled [19, 20]. In our case, we must maximize the success probability over all von Neumann measurements given by orthogonal projectors Π_0 and Π_1 having the same rank n_B. One starts by writing the projector Π_1 as $1 - \Pi_0$ in the expression of the success probability,

$$\begin{aligned} P_S^{\{\Pi_i\}}(\{\rho_i, \eta_i\}) &= \eta_0\,\mathrm{tr}(\Pi_0\rho_0) + \eta_1\,\mathrm{tr}((1-\Pi_0)\rho_1) \\ &= \tfrac{1}{2}(1 - \mathrm{tr}\Lambda) + \mathrm{tr}(\Pi_0\Lambda) \end{aligned} \tag{12}$$

with $\Lambda = \eta_0\rho_0 - \eta_1\rho_1$. Thanks to the min-max principle [31], the maximum of $\mathrm{tr}(\Pi_0\Lambda)$ over all projectors Π_0 of rank n_B is equal to the sum of the n_B highest eigenvalues $\lambda_1 \geqslant \cdots \geqslant \lambda_{n_B}$ of the Hermitian matrix Λ, and the optimal projector $\Pi_0^{\rm opt}$ is the spectral projector associated to these highest eigenvalues. One has

$$P_S^{\text{opt v.N.}}(\{\rho_i, \eta_i\}) = \max_{\{\Pi_i\}} P_S^{\{\Pi_i\}}(\{\rho_i, \eta_i\}) = \frac{1}{2}(1 - \mathrm{tr}\Lambda) + \sum_{l=1}^{n_B} \lambda_l. \tag{13}$$

For the states ρ_i and probabilities η_i defined by equation (9), $\Lambda = \sqrt{\rho}\,(|\alpha_0\rangle\langle\alpha_0| - |\alpha_1\rangle\langle\alpha_1|) \otimes 1\!\!1\sqrt{\rho}$, where $\{|\alpha_i\rangle\}_{i=0}^1$ is an orthonormal basis of $\mathbb{C}^2$. For any such basis the operator inside the parenthesis in the last formula is equal to $\sigma_{\mathbf{u}} \equiv \sum_{m=1}^3 u_m\sigma_m$ for some unit vector $\mathbf{u} \in \mathbb{R}^3$ (here σ_1, σ_2, and σ_3 are the Pauli matrices). Reciprocally, one can associate to any unit vector $\mathbf{u} \in \mathbb{R}^3$ the eigenbasis $\{|\alpha_i\rangle\}_{i=0}^1$ of $\sigma_{\mathbf{u}}$. By substituting (13) into (8), we get

$$F_A(\rho) = \frac{1}{2}\max_{\|\mathbf{u}\|=1}\left\{1 - \mathrm{tr}\Lambda(\mathbf{u}) + 2\sum_{l=1}^{n_B}\lambda_l(\mathbf{u})\right\} \tag{14}$$

where $\lambda_l(\mathbf{u})$ are the eigenvalues in non-increasing order of the $2n_B \times 2n_B$ Hermitian matrix

$$\Lambda(\mathbf{u}) = \sqrt{\rho}\,\sigma_{\mathbf{u}} \otimes 1\!\!1\sqrt{\rho}. \tag{15}$$

Note that $-\rho \leqslant \Lambda(\mathbf{u}) \leqslant \rho$, so that $\sum_{l=1}^{n_B}\lambda_l(\mathbf{u}) \leqslant \sum_{l=1}^{n_B} p_l$, p_l being the eigenvalues of ρ in non-increasing order. If $\rho > 0$ then $\Lambda(\mathbf{u})$ has n_B positive and n_B negative eigenvalues. In such a case (13) reduces to the well-known expression $P_S^{\text{opt v.N.}}(\{\rho_i, \eta_i\}) = P_S^{\rm opt}(\{\rho_i, \eta_i\}) = (1 + \mathrm{tr}|\Lambda(\mathbf{u})|)/2$ [20].

It is shown in [14] that the minimal value that $F_A(\rho)$ can take is equal to $1/n_A$ when $n_A \leqslant n_B$. [6] If A is a qubit, the maximal value of the GQD is thus $D_A = 2 - \sqrt{2}$, see (5). It is convenient to work with a normalized discord, given in terms of $F_A(\rho)$ by

$$\widetilde{D}_A(\rho) = \frac{D_A(\rho)}{2-\sqrt{2}} = \frac{1-\sqrt{F_A(\rho)}}{1-1/\sqrt{2}}. \tag{16}$$

4. Geometric discord in the DQC1 model

In this section, we determine the Bures-GQD for the output state of the DQC1 algorithm. We obtain an analytic expression of the discord for all unitary matrices U_n from which the algorithm computes the trace.

The DQC1 model [11] consists in a control qubit, labelled by the index 0, coupled to n target qubits $1, 2, \ldots, n$. The control qubit is initially in a mixture of the standard basis vectors $|0\rangle$ and $|1\rangle$ with populations $(1 \pm \alpha)/2$ differing from one half. The target qubits are in the completely mixed state $2^{-n}\, 1_n$, where 1_n stands for the identity operator on the 2^n-dimensional space $\mathcal{H}_B$ of qubits $1, \ldots, n$. This state approximates well the thermal state of the nuclear spins in liquid-state nuclear magnetic resonance (NMR) experiments at room temperature. The initial state of the $(n+1)$ qubits reads

$$\rho^{\alpha}_{n+1,\mathrm{in}} = \frac{1}{2^{n+1}}(1 + \alpha\,\sigma_3) \otimes 1_n \tag{17}$$

with $\alpha \in [-1, 1]$, $\alpha \neq 0$. This state is transformed by the following circuit composed of a Hadamard gate H and a unitary gate U_n acting on $\mathcal{H}_B$ controlled by the qubit 0:

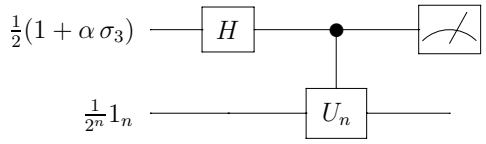

(18)

The output state is

$$\begin{aligned}\rho^{U,\alpha}_{n+1} &= \frac{1}{2^{n+1}}\begin{pmatrix} 1_n & \alpha U_n^{\dagger} \\ \alpha U_n & 1_n \end{pmatrix} \\ &= \frac{1}{2N}\big(|0\rangle\langle 0| \otimes 1_n + |1\rangle\langle 1| \otimes 1_n + \alpha|0\rangle\langle 1| \otimes U_n^{\dagger} + \alpha|1\rangle\langle 0| \otimes U_n\big)\end{aligned} \tag{19}$$

with $N = 2^n$. Hence the reduced state $\mathrm{tr}_{1,\ldots,n}(\rho^{U,\alpha}_{n+1})$ of the qubit 0 contains some information about the normalized trace $z_n = \mathrm{tr}(U_n)/N$. No efficient classical algorithm to compute z_n is known. The DQC1 quantum algorithm provides accurate approximations of $\langle\sigma_1 \otimes 1_n\rangle_{\mathrm{out}} = \alpha\,\mathrm{Re}z_n$ and $\langle\sigma_2 \otimes 1_n\rangle_{\mathrm{out}} = \alpha\,\mathrm{Im}z_n$ after sufficiently many runs of the measurement of the spin σ_1 and σ_2 on the qubit 0. The number of runs is independent of n and scales logarithmically with the error probability. In that sense, the DQC1 algorithm is exponentially more efficient than all known classical algorithms for estimating the *normalized* trace of U_n [12]. Moreover, it works whatever the value of α provided that $\alpha \neq 0$, hence demonstrating the 'power of even the tiniest fraction of a qubit' [12].

The control qubit is unentangled with the target qubits, as can be shown from the relation

$$\rho^{U,\alpha}_{n+1} = \frac{1}{2N}\sum_{k=1}^{N}(|\varphi_k\rangle\langle\varphi_k| + |\chi_k\rangle\langle\chi_k|) \otimes |u_k\rangle\langle u_k|, \tag{20}$$

[6] Moreover, the 'most quantum' states ρ having a minimal fidelity $F_A(\rho)$ are the maximally entangled pure states or convex combinations of such states with reduced B-states having supports on orthogonal subspaces.

where $|u_k\rangle$ are the eigenvectors of U_n with eigenvalues $e^{i\omega_k}$, $|\varphi_k\rangle = \cos\delta|0\rangle + e^{i\omega_k}\sin\delta|1\rangle$, and $|\chi_k\rangle = \sin\delta|0\rangle + e^{i\omega_k}\cos\delta|1\rangle$, with $\sin(2\delta) = \alpha$. For other bipartitions of the $(n+1)$ qubits, e.g., putting together in one subsystem the control qubit and half of the target qubits, the entanglement does not vanish in general but it is bounded uniformly in n [12]. For large system sizes, the total amount of bipartite entanglement is thus a negligible fraction of the maximal entanglement possible.

In what follows, we split the $(n+1)$ qubits into the subsystem A containing the qubit 0 and the subsystem B containing the qubits $1, \ldots, n$. It is clear from (20) that the output state is B-classical, hence it has a vanishing discord δ_B. It was shown in [7] that this state has generically a non-vanishing discord δ_A. The term 'generically' refers here to a random choice of the unitary U_n with the Haar distribution. This presence of a nonzero discord has been demonstrated experimentally in optical [8] and liquid-state NMR [9] implementations of DQC1.

The Bures-GQD of the output state (19) can be easily determined with the help of (14). The eigenvalues of $\rho_{n+1}^{U,\alpha}$ are $(1\pm\alpha)/(2N)$ and the two corresponding eigenspaces are spanned by the N vectors $|0\rangle|\underline{j}\rangle \pm |1\rangle U_n|\underline{j}\rangle$, where $|\underline{j}\rangle$, $\underline{j} \in \{0,1\}^n$, are the standard basis vectors of $\mathcal{H}_B$. This yields the square root

$$\sqrt{\rho_{n+1}^{U,\alpha}} = \frac{1}{\sqrt{2N}} V \begin{pmatrix} \sqrt{1+\alpha}\,1_n & 0 \\ 0 & \sqrt{1-\alpha}\,1_n \end{pmatrix} V^\dagger, \quad V = \frac{1}{\sqrt{2}} \begin{pmatrix} 1_n & 1_n \\ U_n & -U_n \end{pmatrix}. \tag{21}$$

Substituting this expression into (15) and introducing the angles θ, ϕ such that $\mathbf{u} = (\sin\theta\cos\phi, \sin\theta\sin\phi, \cos\theta)$, one finds

$$\Lambda(\mathbf{u}) = \frac{1}{2N} V \begin{pmatrix} (1+\alpha)\sin\theta\,\mathrm{Re}\big(U_n^\phi\big) & \sqrt{1-\alpha^2}\big(\cos\theta - i\sin\theta\,\mathrm{Im}\big(U_n^\phi\big)\big) \\ \sqrt{1-\alpha^2}\big(\cos\theta + i\sin\theta\,\mathrm{Im}\big(U_n^\phi\big)\big) & -(1-\alpha)\sin\theta\,\mathrm{Re}\big(U_n^\phi\big) \end{pmatrix} V^\dagger \tag{22}$$

with $U_n^\phi = e^{-i\phi}U_n$. Here, $\mathrm{Re}(O) = (O+O^\dagger)/2$ and $\mathrm{Im}(O) = (O-O^\dagger)/2i$ denote the real and imaginary parts of the operator O. By diagonalizing each of the four blocks of the matrix appearing between V and $V^\dagger$ in the right-hand side of (22), one sees that its eigenvalues $\lambda_{k,\pm}(\mathbf{u})$ are the eigenvalues of k distinct 2×2 matrices. This yields

$$\lambda_{k,\pm}(\mathbf{u}) = \frac{1}{2N}\left(\alpha\sin\theta\cos\left(\omega_k^\phi\right) \pm \sqrt{1-\alpha^2+\alpha^2\sin^2\theta\cos^2\left(\omega_k^\phi\right)}\right) \tag{23}$$

for $k = 1, \ldots, N$, where $\omega_k^\phi = \omega_k - \phi$ are the eigenphases of U_n^ϕ. One has clearly $\pm\lambda_{k,\pm}(\mathbf{u}) \geqslant 0$. Writing the maximum over $\mathbf{u}$ in (14) as a maximum over θ and ϕ and noting that the maximum over θ is reached for $\sin^2\theta = 1$, we get

$$F_A\big[\rho_{n+1}^{U,\alpha}\big] = \frac{1}{2}\max_\phi\left\{1 + \frac{1}{N}\sum_{k=1}^{N}\sqrt{1-\alpha^2\sin^2(\omega_k-\phi)}\right\}. \tag{24}$$

Let us point out that the maximal fidelity (24) to the A-classical states is a decreasing function of α^2. Hence the geometric discord $D_A(\rho_{n+1}^{U,\alpha})$ increases with the initial purity $(1+\alpha^2)/2$ of the control qubit.

For large system sizes n, the sum over k in (24) can be replaced by an integral over the smooth normalized spectral density $n(\omega)$ of the eigenphases ω_k of U_n,

$$F_A\big[\rho_{n+1}^{U,\alpha}\big] = \frac{1}{2}\max_\phi\left\{1 + \int_0^{\frac{\pi}{2}} d\omega\,\sqrt{1-\alpha^2\sin^2\omega}\,(n_S(\omega+\phi) + n_S(\pi-\omega+\phi))\right\} \tag{25}$$

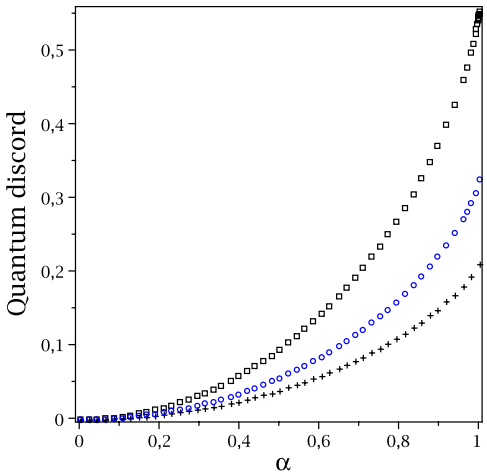

Figure 1. QDs of the output state in the DQC1 algorithm as a function of the purity parameter α. From top to bottom: discord δ_A for random unitaries U_n distributed according to the Haar measure in the limit $n \to \infty$ (black squares); normalized Bures-GQD $\widetilde{D}_A$ for the same choice of unitaries (blue circles); normalized Bures-GDQ for the rotation matrices (28) (black crosses).

with $n_S(\omega) = n(\omega) + n(\omega + \pi)$. Let us show that the smallest fidelity is achieved for unitary operators U_n having a constant symmetrized spectral density $n_S(\omega) = 1/\pi$. Actually, by substituting $\max_\phi$ by $\int_0^{2\pi} \mathrm{d}\phi/(2\pi)$ in (25) and using $\int_0^{2\pi} \mathrm{d}\phi\, n_S(\phi) = 2$, one gets the bound

$$F_A\big[\rho_{n+1}^{U,\alpha}\big] \geqslant F_A\big[\rho_{n+1}^{U_{\mathrm{unif}},\alpha}\big] = \frac{1}{2}\left(1 + \frac{2}{\pi}\int_0^{\frac{\pi}{2}} \mathrm{d}\omega\, \sqrt{1-\alpha^2\sin^2\omega}\right). \tag{26}$$

The inequality is an equality if and only if the integral in (25) is independent of ϕ. Expanding n_S as a Fourier series, $n_S(\omega) = \sum_p a_p \mathrm{e}^{2\mathrm{i}p\omega}$, this is equivalent to

$$\sum_{p=-\infty}^{\infty} p a_p\, \mathrm{e}^{2\mathrm{i}p\phi} \int_0^{\frac{\pi}{2}} \mathrm{d}\omega\, \sqrt{1-\alpha^2\sin^2\omega}\, \cos(2p\omega) = 0 \tag{27}$$

for any $\phi \in [0, 2\pi[$. For $\alpha = 1$, one easily sees that the integrals in (27) do not vanish for any p. Therefore $a_p = 0$ when $p \neq 0$ and $n_S(\omega)$ is constant. Reciprocally, if $n_S(\omega)$ is constant then for any $\alpha \in [-1, 1]$ the inequality in (26) is an equality.

Let us emphasize that the bound (26) is satisfied for all $n \geqslant 1$ (in fact, it can be obtained by replacing as before the maximum over ϕ by an integral, but in equation (24) instead of (25)). As a consequence, whatever the unitary matrix U_n and the system size n, the GQD is always smaller or equal to the GQD for an infinite unitary matrix U_{unif} with constant symmetrized spectral density n_S. Such matrices have equidistributed eigenvalues on the unit circle modulo a symmetry with respect to the origin. This highest possible discord is achieved in particular for random unitaries distributed according to the Haar measure on the unitary group $U(N)$, since then $n(\omega) = 1/(2\pi)$ almost surely in the large n limit [7].

The normalized GQD (16) of the output state (19) is shown in figure 1 as a function of α for the optimal unitaries U_{unif} with constant $n_S(\omega)$ and for the rotation operator

$$U_n = \exp\left(\frac{\mathrm{i}\pi}{2\sqrt{n}}(J_z)_n\right), \quad n \gg 1, \tag{28}$$

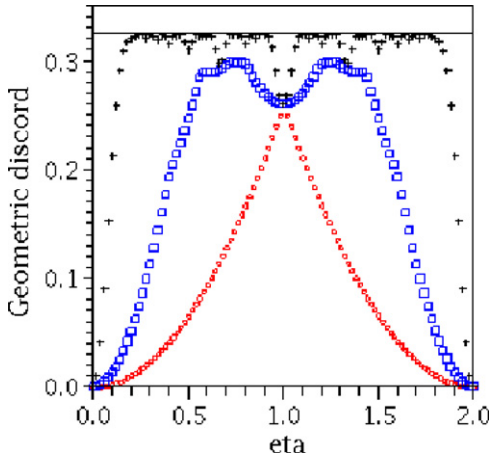

Figure 2. Normalized discord $\widetilde{D}_A$ of the output state in the DQC1 algorithm for $U_n(\eta) = \exp[\mathrm{i}\frac{\pi}{2}\eta(J_z)_n]$ as a function of η. The control qubit is initially in a pure state ($\alpha = 1$). From top to bottom: $n = 100$ (black crosses), $n = 5$ (blue squares), and $n = 1$ (red diamonds). All discords are periodic with period 2 (not shown) and symmetric with respect to $\eta = 1$. The horizontal line gives the maximal value $\widetilde{D}_A = (1 - \sqrt{1/2 + 1/\pi})/(1 - 1/\sqrt{2})$ obtained for random unitaries as in figure 1.

where $(J_z)_n = \sum_{i=1}^n \sigma_3^{(i)}/2$ is the total angular momentum of the n spins in the z direction. In the second case, the fidelity is determined from equation (24) by using the non-periodic spectral density $n(\omega) = (2/\pi)^{3/2}\exp(-8\,\omega^2/\pi^2)$ and noting that the maximum is reached for $\phi = 0$. This Gaussian density is obtained by using the fact that the eigenphases of U_n, $\omega_k = \pi(k - n/2)/(2\sqrt{n})$ with $k = 0, \ldots, n$, have multiplicities $d_k = \frac{n!}{k!(n-k)!}$ satisfying $2^{-n}d_k \sim \sqrt{\frac{2}{\pi n}}\exp[-2(k - \frac{n}{2})^2/n]$ in the limit $n \to \infty$ (note that the scaling like $1/\sqrt{n}$ of the rotation angle in (28) is dictated by the wish to obtain a nontrivial $n(\omega)$). We also compare in figure 1 the geometric discord with the QD (3), using the result of [7] applying to random unitaries with the Haar distribution. We observe that $\delta_A(\rho_{n+1}^{U,\alpha}) \geqslant \widetilde{D}_A(\rho_{n+1}^{U,\alpha})$.

Finally, let us determine the unitaries U_n leading to the smallest discord. The fidelity (24) takes its maximal value 1 when $\mathrm{e}^{\mathrm{i}\omega_k} \in \{\mathrm{e}^{\mathrm{i}\phi}, -\mathrm{e}^{\mathrm{i}\phi}\}\ \forall\ k = 1, \ldots, N$, for a fixed angle $\phi \in [0, 2\pi[$. Hence $D_A(\rho_{n+1}^{U,\alpha}) = 0$ if and only if $U_n = \mathrm{e}^{\mathrm{i}\phi}Q$ with $\phi \in [0, 2\pi[$, $Q = Q^\dagger$, and $Q^2 = Q$. Figure 2 displays the GQD for finite system sizes n. In agreement with the aforementioned criterion, the discord vanishes for rotation matrices U_n with rotation angles equal to 0 or π. Moreover, it is independent of n when the rotation angle is equal $\pi/2$. The existence of output states of the DQC1 model with a zero-discord and the necessary and sufficient condition stated above have already been discussed in [13]. Let us notice that the particular matrices U_n which have been conjectured in [12] to lead for $\alpha = 1$ to the highest possible bipartite entanglement among the $(n + 1)$ qubits satisfy this condition. For such U_n the discord between the control qubit and the n target qubits thus vanishes.

5. Two-qubit states with maximally mixed marginals

This section is devoted to the determination of the geometric discord D_A and the closest A-classical states for two-qubit systems. With the aim of comparing D_A with the other QDs, we consider a simple convex family of two-qubit density matrices for which all discords can

be easily calculated: the states ρ with maximally mixed marginals $\rho_A = \rho_B = 1/2$. Any such state can be written up to a conjugation by a local unitary $U_A \otimes U_B$ (which leaves all discords unchanged) as [32]

$$\rho = \frac{1}{4}\left(1 \otimes 1 + \sum_{m=1}^{3} c_m \sigma_m \otimes \sigma_m\right) \tag{29}$$

where the real vector $\mathbf{c} = (c_1, c_2, c_3)$ belongs to the tetrahedron with vertices $F_\pm = (\pm 1, \mp 1, 1)$ and $G_\pm = (\pm 1, \pm 1, -1)$, that is,

$$\begin{aligned} p_0 &= \tfrac{1}{4}(1 - c_1 - c_2 - c_3) \geqslant 0, \\ p_m &= \tfrac{1}{4}(1 + c_1 + c_2 + c_3 - 2c_m) \geqslant 0, \quad m = 1, 2, 3. \end{aligned} \tag{30}$$

The vertices $F_\pm$ and $G_\pm$ correspond to the Bell states $|\Phi^\pm\rangle = (|00\rangle \pm |11\rangle)/\sqrt{2}$ and $|\Psi^\pm\rangle = (|01\rangle \pm |10\rangle)/\sqrt{2}$, respectively. The non-negative numbers p_ν are the probabilities of these four Bell states in $\rho = \sum_{\nu=0}^{3} p_\nu |\Psi_\nu\rangle\langle\Psi_\nu|$, with $|\Psi_0\rangle = |\Psi^-\rangle$, $|\Psi_1\rangle = |\Phi^-\rangle$, $|\Psi_2\rangle = |\Phi^+\rangle$, and $|\Psi_3\rangle = |\Psi^+\rangle$. The states (29) form a 3-parameter convex subset $\mathcal{T}$ in the 15-parameter set $\mathcal{E}$ of all two-qubit states.

5.1. Explicit formula for the GQD

Let us calculate $D_A(\rho)$ for two qubits in the state (29). The matrices ρ and $\sqrt{\rho}$ are given in the standard basis $\{|00\rangle, |10\rangle, |01\rangle, |11\rangle\}$ by

$$\rho = \frac{1}{4}\begin{pmatrix} 1 + c_3 & 0 & 0 & c_1 - c_2 \\ 0 & 1 - c_3 & c_1 + c_2 & 0 \\ 0 & c_1 + c_2 & 1 - c_3 & 0 \\ c_1 - c_2 & 0 & 0 & 1 + c_3 \end{pmatrix} \tag{31}$$

and

$$\sqrt{\rho} = \begin{pmatrix} t_0 + t_3 & 0 & 0 & t_1 - t_2 \\ 0 & t_0 - t_3 & t_1 + t_2 & 0 \\ 0 & t_1 + t_2 & t_0 - t_3 & 0 \\ t_1 - t_2 & 0 & 0 & t_0 + t_3 \end{pmatrix} \tag{32}$$

where

$$4t_0 = \sqrt{p_0} + \sqrt{p_1} + \sqrt{p_2} + \sqrt{p_3}, \quad 4t_1 = -\sqrt{p_0} - \sqrt{p_1} + \sqrt{p_2} + \sqrt{p_3}, \tag{33}$$

with similar formulas for t_2 and t_3 obtained by permutation of the indices 1, 2, 3. The real parameters t_ν satisfy $4(t_0^2 + t_1^2 + t_2^2 + t_3^2) = \mathrm{tr}\rho = 1$. Let θ and ϕ be the angles defined by the vector $\mathbf{u} = (\sin\theta\cos\phi, \sin\theta\sin\phi, \cos\theta)$ on the unit sphere. In the standard basis, the matrix $\Lambda(\mathbf{u}) = \sqrt{\rho}\,\sigma_\mathbf{u} \otimes 1\sqrt{\rho}$ reads

$$\Lambda(\mathbf{u}) = \frac{1}{4}\begin{pmatrix} (a_3 + b_3)\cos\theta & \zeta_\phi^* \sin\theta & \xi_\phi^* \sin\theta & 0 \\ \zeta_\phi \sin\theta & (a_3 - b_3)\cos\theta & 0 & \xi_\phi^* \sin\theta \\ \xi_\phi \sin\theta & 0 & (-a_3 + b_3)\cos\theta & \zeta_\phi^* \sin\theta \\ 0 & \xi_\phi \sin\theta & \zeta_\phi \sin\theta & (-a_3 - b_3)\cos\theta \end{pmatrix} \tag{34}$$

with $\xi_\phi = a_1 \cos\phi + \mathrm{i}a_2 \sin\phi$, $\zeta_\phi = b_1 \cos\phi + \mathrm{i}b_2 \sin\phi$, and

$$b_m = 8\big(t_0^2 + t_m^2\big) - 1, \quad a_1 = 8(t_0 t_1 + t_2 t_3), \quad a_2 = 8(t_0 t_2 + t_1 t_3), \quad a_3 = 8(t_0 t_3 + t_1 t_2). \tag{35}$$

One finds

$$a_3 = 2\big(-\sqrt{p_0 p_3} + \sqrt{p_1 p_2}\big), \quad b_3 = 2\big(\sqrt{p_0 p_3} + \sqrt{p_1 p_2}\big). \tag{36}$$

Similar expressions hold for the other coefficients a_1, a_2, b_1, and b_2 by permuting the indices 1, 2, 3.

The eigenvalues of $\Lambda(\mathbf{u})$ come in opposite pairs $(\lambda_\pm(\mathbf{u}), -\lambda_\pm(\mathbf{u}))$ with

$$\lambda_\pm(\mathbf{u}) = \tfrac{1}{4}\left|\sqrt{b_3^2\cos^2\theta + |\zeta_\phi|^2\sin^2\theta} \pm \sqrt{a_3^2\cos^2\theta + |\xi_\phi|^2\sin^2\theta}\right|, \tag{37}$$

in agreement with $\mathrm{tr}\Lambda(\mathbf{u}) = \mathrm{tr}(\rho_A\sigma_\mathbf{u}) = 0$. But $|a_m| \leqslant b_m$ by (36), thus the second square root is smaller than the first one. One deduces from (14) that

$$F_A(\rho) = \tfrac{1}{2}\left(1 + \max_{\theta,\phi}\sqrt{b_3^2\cos^2\theta + \left(b_1^2\cos^2\phi + b_2^2\sin^2\phi\right)\sin^2\theta}\right). \tag{38}$$

If the b_m are distinct from each other, the maximum is reached for $\cos^2\theta, \cos^2\phi \in \{0, 1\}$, that is, for $\mathbf{u} = \pm\mathbf{e}_1, \pm\mathbf{e}_2$, or $\pm\mathbf{e}_3$ (here $\mathbf{e}_m$ are the coordinate axis vectors). If $b_1 = b_2 > b_3$, this maximum is reached for $\mathbf{u} = \cos\phi\,\mathbf{e}_1 + \sin\phi\,\mathbf{e}_2$ with $\phi \in [0, 2\pi[$ arbitrary. Thus

$$F_A(\rho) = \frac{1 + b_{\max}}{2} \quad \text{and} \quad \widetilde{D}_A(\rho) = \left(1 - \frac{1}{\sqrt{2}}\right)^{-1}\left(1 - \sqrt{\frac{1 + b_{\max}}{2}}\right) \tag{39}$$

with

$$\begin{aligned} b_{\max} = \max_{m=1,\ldots,3}\{b_m\} = \tfrac{1}{2}\max\Big\{&\sqrt{(1+c_1)^2 - (c_2 - c_3)^2} + \sqrt{(1-c_1)^2 - (c_2 + c_3)^2}, \\ &\sqrt{(1+c_2)^2 - (c_1 - c_3)^2} + \sqrt{(1-c_2)^2 - (c_1 + c_3)^2}, \\ &\sqrt{(1+c_3)^2 - (c_1 - c_2)^2} + \sqrt{(1-c_3)^2 - (c_1 + c_2)^2}\Big\}. \end{aligned} \tag{40}$$

We notice that if $|c_m|$ is maximum for $m = m_{\max}$ then this is also true for b_m, i.e., the maximal number inside the brackets in (40) is the $(m_{\max})$th one. Actually, one can show from (36) and (30) that

$$c_m^2 - c_k^2 = b_m^2 - b_k^2, \quad m, k = 1, \ldots, 3. \tag{41}$$

It is clear on (40) that the vectors $\mathbf{c}$ such that $b_{\max}$ takes the highest possible value $b_{\max} = 1$ have a single non-vanishing component c_m. Therefore, in agreement with the results of [13], the A-classical states with maximally mixed marginals are located (up to local unitary equivalence) on the three segments of the coordinate axes inside the tetrahedron, represented in figure 3(*a*) by thick dashed lines. As a consequence, all states ρ such that $\mathbf{c}$ is inside the octahedron formed by the convex hull of the three aforementioned segments are separable (for indeed, convex combinations of A-classical states are separable). It follows from the Peres–Horodecki criterion that this octahedron contains all separable states with maximally mixed marginals [32].

The states (29) with the highest discord $\widetilde{D}_A = 1$ have $b_1 = b_2 = b_3 = 0$. These states are the four Bell states $|\Psi_\nu\rangle$ located at the vertices $F_\pm$ and $G_\pm$ of the tetrahedron (see figure 3(*a*)). Note that an analogous result holds for the Hilbert–Schmidt-GQD [13].

Let us end this subsection by remarking that for two-qubit states ρ with maximally mixed marginals $\rho_A = \rho_B = 1/2$, the inequality (10) is an equality. Actually, for such ρ one has equal prior probabilities $\eta_i = \langle\alpha_i|\rho_A|\alpha_i\rangle = 1/2$ in the QSD task of section 2.3. Moreover, it follows from (29) that ρ is invariant under conjugation by the spin-flip operators $\sigma_1 \otimes \sigma_1$ and $\sigma_2 \otimes \sigma_2$. But it has been observed above that an optimal direction $\mathbf{u}^{\mathrm{opt}}$ is given by one of the coordinate vectors $\mathbf{e}_m$ or its opposite. Disregarding irrelevant phase factors, the two eigenvectors $|\alpha_0^{\mathrm{opt}}\rangle$ and $|\alpha_1^{\mathrm{opt}}\rangle$ of $\sigma_{\mathbf{u}^{\mathrm{opt}}}$ are transformed one into another by the spin-flip operator σ_m, with $m = 1$ if $\mathbf{u}^{\mathrm{opt}} = \pm\mathbf{e}_2, \pm\mathbf{e}_3$ and/or $m = 2$ if $\mathbf{u}^{\mathrm{opt}} = \pm\mathbf{e}_1, \pm\mathbf{e}_3$. Hence the states ρ_i are related by a unitary conjugation, $\rho_1 = \sigma_m \otimes \sigma_m\,\rho_0\,\sigma_m \otimes \sigma_m$. The square-root measurement is known to be optimal to discriminate such symmetric ensembles of states with equal prior probabilities [26, 27]. Thus $F_A(\rho)$ is given by the right-hand side of equation (10). Based on this observation, one can rederive formula (39) in a slightly simpler way.

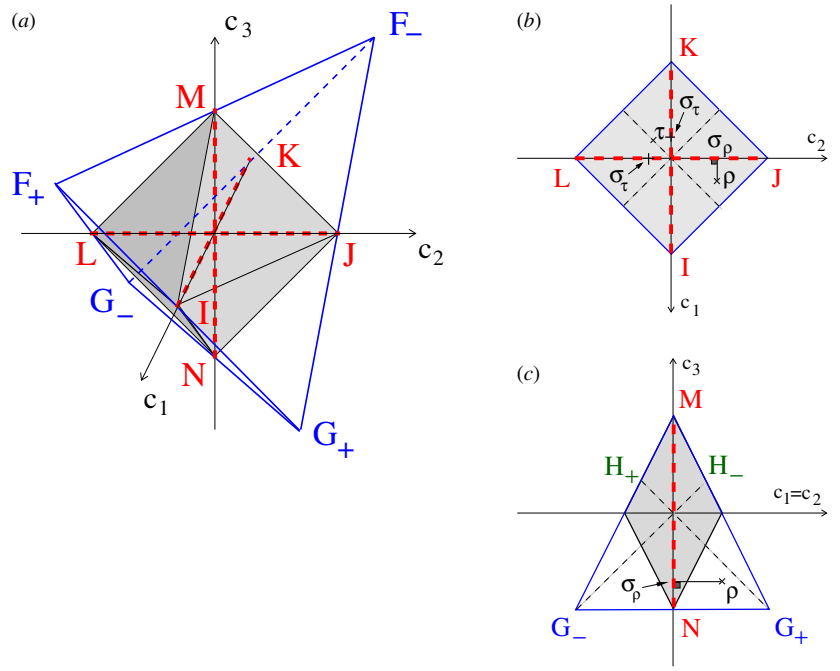

Figure 3. (*a*) Tetrahedron $\mathcal{T}$ with vertices $F_\pm = (\pm 1, \mp 1, 1)$ and $G_\pm = (\pm 1, \pm 1, -1)$, and center $O(0, 0, 0)$. The vectors $\mathbf{c} \in \mathcal{T}$ represent physical states $\rho(\mathbf{c})$ with maximally mixed marginals. The A-classical states in $\mathcal{T}$ are also B-classical and are located on the segments $[IK]$, $[JL]$, and $[MN]$ (thick red dashed lines), with $I(1, 0, 0)$, $J(0, 1, 0)$, $K(-1, 0, 0)$, $L(0, -1, 0)$, $M(0, 0, 1)$, and $N(0, 0, -1)$. The shaded region delimited by the octahedron $IJKLMN$ corresponds to separable states. (*b*) Cut view of $\mathcal{T}$ in the plane $c_3 = 0$. The state $\rho(\frac{1}{4}, \frac{1}{2}, 0)$ has a unique closest classical state (CCS) $\sigma_\rho(0, s_2, 0)$ with $s_2 \simeq 0.523$ (see equation (47)). States on the broken lines are at equal Bures distance from the segments $[IK]$ and $[JL]$ and have infinitely many CCSs, given by equation (51). On these lines $D_A(\rho)$ is not differentiable. Two CCSs of the form (29) to the state $\tau(-\frac{1}{4}, -\frac{1}{4}, 0)$, corresponding to $\mathbf{u} = \mathbf{e}_1$ and $\mathbf{e}_2$ in (51), are shown: $\sigma_\tau(s_1, 0, 0)$ and $\sigma_\tau(0, s_1, 0)$ with $s_1 \simeq -0.259$. (*c*) Cut view of $\mathcal{T}$ in the plane $c_1 = c_2$. States in the shaded region are separable. The state $\rho(\frac{1}{2}, \frac{1}{2}, -\frac{3}{4})$ has a unique CCS $\sigma_\rho(0, 0, s_3)$, with $s_3 \simeq -0.729$. States inside the triangles $H_\mp OG_\pm$ have infinitely many CCSs, given by (51). All states lying on the blue edges of the square and triangle in panels (*b*) and (*c*), and on the faces of $\mathcal{T}$ in panel (*a*), have infinitely many CCSs, given by equations (55) and (56).

5.2. Comparison with the other discords

We can now compare the normalized GQD $\widetilde{D}_A(\rho)$ for states ρ of the form (29) with other measures of QCs. The corresponding QD

$$\delta_A(\rho) = \sum_{\nu=0}^{3} p_\nu \ln_2 p_\nu + 2 - \frac{1 - |\mathbf{c}|}{2} \ln_2(1 - |\mathbf{c}|) - \frac{1 + |\mathbf{c}|}{2} \ln_2(1 + |\mathbf{c}|) \quad (42)$$

has been calculated in [33]. Here, $|\mathbf{c}| = \max_m |c_m|$ and the probabilities p_ν are given by (30). The GQD with Hilbert–Schmidt distance, $D_A^{(2)}(\rho) = d_2(\rho, \mathcal{C}_A)^2 \equiv \min_{\sigma \in \mathcal{C}_A} \mathrm{tr}[(\rho - \sigma)^2]$, is easy to determine for arbitrary two-qubit states [13]. For the states (29) it reads $D_A^{(2)}(\rho) = (\sum_m c_m^2 - |\mathbf{c}|^2)/4$. Since the maximal value of $D_A^{(2)}$ is $1/2$, we normalize it as $\widetilde{D}_A^{(2)}(\rho) = 2D_A^{(2)}(\rho)$. A third discord considered in [34] is defined with the help of the relative entropy $S(\rho||\sigma) = \mathrm{tr}(\rho \ln \rho) - \mathrm{tr}(\rho \ln \sigma)$ as $\Delta_A(\rho) = \min_{\sigma \in \mathcal{C}_A} S(\rho||\sigma)$.

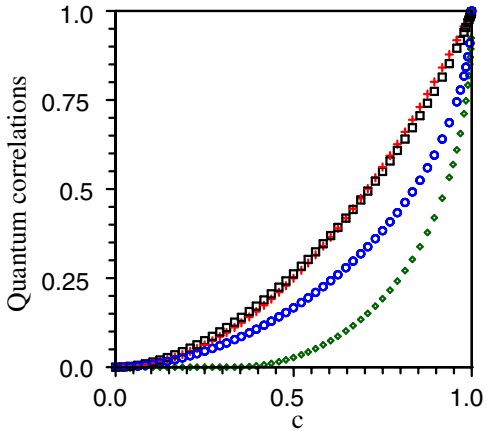

Figure 4. Comparison of the normalized discords and geometric entanglement for a Werner state $\rho_W = \frac{1-c}{4}\,1 + c|\Psi^-\rangle\langle\Psi^-|$ with c varying between 0 and 1 (ρ_W is located on the segment $[OG_-]$ in figure 3(*a*)). From top to bottom: QD δ_A (black boxes), GQD $\widetilde{D}_A^{(2)}$ with Hilbert–Schmidt distance (red crosses), GQD $\widetilde{D}_A$ with Bures distance (blue circles), and geometric measure of entanglement $\widetilde{E}$ (green diamonds).

However, for the states (29) it coincides with $\delta_A(\rho)$ [18]. We also compare $\widetilde{D}_A(\rho)$ with the geometric measure of entanglement (see section 2.2), given for two qubits by $E(\rho) = 2 - \sqrt{2}(1 + \sqrt{1 - C(\rho)^2})^{1/2}$ [16] where $C(\rho)$ is the Wootters concurrence [35]. In our case $C(\rho) = \max\{|c_1 - c_2| - 1 + c_3, |c_1 + c_2| - 1 - c_3, 0\}/2$. The measure E is normalized as $\widetilde{E}(\rho) = E(\rho)/(2 - \sqrt{2})$. Let us point out that $\widetilde{E}(\rho) \leqslant \widetilde{D}_A(\rho)$ for any ρ, since A-classical states are separable.

In figure 4, the four QC measures $\widetilde{D}_A$, δ_A, $\widetilde{D}_A^{(2)}$, and $\widetilde{E}$ are plotted together for the Werner states, obtained by taking $c_1 = c_2 = c_3 = -c$ in (29), with $0 \leqslant c \leqslant 1$.

Figure 5(*a*) displays the difference $\widetilde{D}_A(\rho) - \delta_A(\rho)$ for a subfamily of states with maximally mixed marginals depending on two parameters. We observe that

$$\delta_A(\rho) \geqslant \widetilde{D}_A(\rho). \tag{43}$$

In contrast, one sees in figures 4 and 5(*b*) that the GQD with Hilbert–Schmidt distance can be either smaller or larger than δ_A, as it has been noted previously in other works [36]. We have looked numerically for vectors $\mathbf{c}$ inside the tetrahedron violating (43) and have not found any such vector. This indicates that this bound holds for any state ρ with maximally mixed marginals. It would be of interest to know if it also holds for more general states. Let us recall from section 4 that (43) is true for the output state of the DQC1 model with random unitaries.

5.3. Closest A-classical states

We now turn to the problem of finding the A-classical states σ_ρ satisfying

$$d_B(\rho, \sigma_\rho)^2 = D_A(\rho) = \min_{\sigma_{A\text{-cl}} \in \mathcal{C}_A} d_B(\rho, \sigma_{A\text{-cl}})^2. \tag{44}$$

These closest A-classical states to ρ provide useful information on ρ and on the geometry of the set of quantum states. Such information, which is not contained in the discord $D_A(\rho)$, can be of interest when studying dynamical evolutions, for instance, when the two subsystems are coupled to their environments and undergo decoherence processes. Like in the two

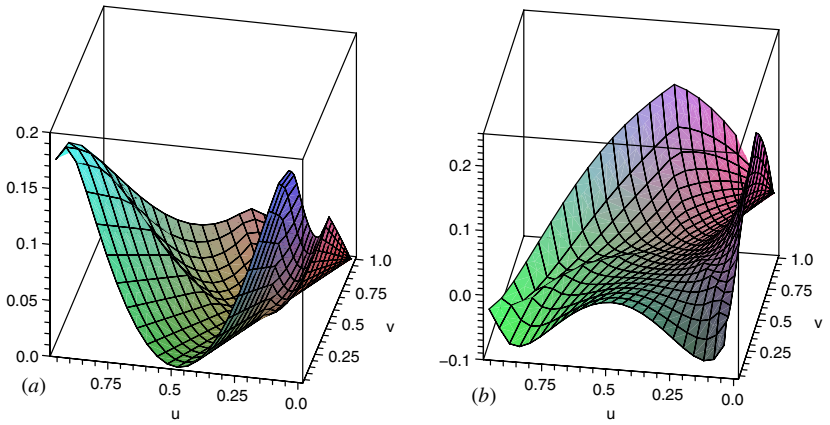

Figure 5. (*a*) Difference $\delta_A(\rho) - \widetilde{D}_A(\rho)$ between the QD and the normalized Bures-GQD for states with maximally mixed marginals with vectors $\mathbf{c}$ inside the triangle of vertices F_+, F_-, and N (see figure 3(*a*)). The parameters u and v, $0 \leqslant u \leqslant 1 - v \leqslant 1$, are chosen such that $c_1 = -2u - v + 1 = -c_2$ and $c_3 = -2v + 1$; (*b*) same for the difference $\delta_A(\rho) - \widetilde{D}_A^{(2)}(\rho)$ between the QD and the normalized Hilbert–Schmidt-GQD.

previous subsections, we focus on two-qubit states with maximally mixed marginals given by equation (29). The geometric representation of these states by vectors $\mathbf{c}$ in the tetrahedron $\mathcal{T}$ will give some insight to our results. In order to compare the geometries on $\mathcal{T}$ associated to the two distances d_B and d_2, we also determine the closest A-classical states for the Hilbert–Schmidt distance d_2 by using the results of [13].

The states σ_ρ are obtained by applying formula (11). In view of the results of section 3, the optimal basis $\{|\alpha_i^{\rm opt}\rangle\}_{i=0}^1$ is the eigenbasis of the spin operator $\sigma_{\mathbf{u}^{\rm opt}}$ in the optimal direction $\mathbf{u}^{\rm opt}$. We already know that for the states (29), $\mathbf{u}^{\rm opt}$ is parallel to the coordinate vector $\mathbf{e}_{m_{\max}}$ if the maximum $|\mathbf{c}| = \max_{m=1,2,3} |c_m|$ is reached for a single index $m = m_{\max}$ (see section 5.1); otherwise, $\mathbf{u}^{\rm opt}$ is an arbitrary unit vector in the space spanned by the $\mathbf{e}_m$ corresponding to indices m such that $|c_m| = |\mathbf{c}|$ (indeed, for such indices the parameters b_m in (38) are equal, $b_m = b_{\max}$, by virtue of (41)). Moreover, it has been shown in section 5.1 that the states $\rho_i^{\rm opt}$ are optimally discriminated by the square-root measurement given by the projectors

$$\Pi_i^{\rm opt} = |\alpha_i^{\rm opt}\rangle\langle\alpha_i^{\rm opt}| \otimes 1. \tag{45}$$

Let us first take $\mathbf{u}^{\rm opt} = \pm\mathbf{e}_{m_{\max}}$. Then $\sigma_{m_{\max}} = \pm(|\alpha_0^{\rm opt}\rangle\langle\alpha_0^{\rm opt}| - |\alpha_1^{\rm opt}\rangle\langle\alpha_1^{\rm opt}|)$. One infers from the expression (32) of the matrix $\sqrt{\rho}$ in the standard basis that $\sqrt{\rho} = \sum_{\nu=0}^3 t_\nu \sigma_\nu \otimes \sigma_\nu$, where t_ν are given by (33) and we have set $\sigma_0 = 1$. This yields

$$\langle\alpha_i^{\rm opt}|\sqrt{\rho}|\alpha_i^{\rm opt}\rangle = t_0 \pm (-1)^i t_{\max}\sigma_{m_{\max}} \tag{46}$$

with $t_{\max} \equiv t_{m_{\max}}$. Replacing (45) and (46) into (11) and using the identities $F_A(\rho) = 4(t_0^2 + t_{\max}^2)$ and $16 t_0 t_m = a_m + c_m$, which follow respectively from (39) and (35) and from (33), (30), and (36), one finds

$$\sigma_\rho = \frac{1}{4}\left(1 \otimes 1 + \frac{a_{m_{\max}} + c_{m_{\max}}}{2F_A(\rho)}\,\sigma_{m_{\max}} \otimes \sigma_{m_{\max}}\right) \tag{47}$$

where

$$a_1 = 2\big(-\sqrt{p_0 p_1} + \sqrt{p_2 p_3}\big) = \tfrac{1}{2}\Big(\sqrt{(1+c_1)^2 - (c_2 - c_3)^2} - \sqrt{(1-c_1)^2 - (c_2 + c_3)^2}\Big), \tag{48}$$

with analogous formulas for a_2 and a_3 obtained via a permutation of indices. Hence, a two-qubit state ρ with maximally mixed marginals always admits among its closest A-classical states a state with maximally mixed marginals, given by equation (47). This closest state has the following decomposition in terms of the four Bell states

$$\sigma_\rho = \frac{1-q_{m_{\max}}}{2}\sum_{\nu=0,m_{\max}} |\Psi_\nu\rangle\langle\Psi_\nu| + \frac{q_{m_{\max}}}{2}\sum_{\nu\neq 0,m_{\max}} |\Psi_\nu\rangle\langle\Psi_\nu| \tag{49}$$

with

$$q_m = \frac{(t_0+t_m)^2}{2\left(t_0^2+t_m^2\right)} = \frac{1}{2} + \frac{a_m+c_m}{2b_m+2}. \tag{50}$$

Interestingly, the closest states (49) for the Bures distance have the same form as the closest states for the relative entropy. Actually, the states σ_ρ^Δ satisfying $S(\rho||\sigma_\rho^\Delta) = \min_{\sigma\in\mathcal{C}_A} S(\rho||\sigma)$ are given by equation (49) but with different probabilities $q_{m_{\max}}$ and $1-q_{m_{\max}}$, given by the sums of the two largest or the two smallest probabilities p_ν [34]. According to our notation, these two smallest (respectively largest) probabilities are p_0 and $p_{m_{\max}}$ if $|c_m| = |\mathbf{c}|$ for a single index $m = m_{\max}$ and $p_0 + p_{m_{\max}} < 1/2$ (respectively $p_0 + p_{m_{\max}} > 1/2$).

If $|c_m| = |\mathbf{c}|$ for two indices m, say, $|c_1| = |c_2| > |c_3|$ with $c_1 = \pm c_2$, all the eigenbasis $\{|\alpha_{\phi,i}^{\text{opt}}\rangle\}$ of the spin operators $\sigma_\phi = \cos\phi\,\sigma_1 + \sin\phi\,\sigma_2$ maximize the success probability $P_S^{\text{opt v.N.}}(\{\rho_i,\eta_i\})$ in (8). Hence ρ has infinitely many closest A-classical states σ_ρ. These states can be determined by a simple generalization of the calculation leading to (47), choosing for Π_i^{opt} the square-root measurement operators (45) associated to $\{|\alpha_{\phi,i}^{\text{opt}}\rangle\}$. Let us note that $c_1 = \pm c_2$ implies $t_1 = \pm t_2$ and recall the identities $|\alpha_{\phi,i}^{\text{opt}}\rangle = \mathrm{e}^{-i\frac{\phi}{2}\sigma_3}|\alpha_{0,i}^{\text{opt}}\rangle$ and $\mathrm{e}^{\mathrm{i}\frac{\phi}{2}\sigma_3}\sigma_{\mathbf{u}}\,\mathrm{e}^{-\mathrm{i}\frac{\phi}{2}\sigma_3} = \sigma_{\mathbf{u}'}$, where $\mathbf{u}'$ is related to $\mathbf{u}$ by a rotation around the z-axis with the angle $-\phi$. We find the following family of A-classical closest states depending on the optimal vector $\mathbf{u} = u_1\,\mathbf{e}_1 + u_2\,\mathbf{e}_2$ with $u_1^2 + u_2^2 = 1$:

$$\sigma_\rho(\mathbf{u}) = \frac{1}{4}\left(1\otimes 1 + \frac{a_{m_{\max}}+c_{m_{\max}}}{2F_A(\rho)}\,\sigma_{\mathbf{u}}\otimes\sigma_{\mathbf{u}(\mathbf{c})}\right) \tag{51}$$

with $m_{\max}\in\{1,2\}$ and $\mathbf{u}(\mathbf{c}) = c_{m_{\max}}^{-1}(c_1u_1\,\mathbf{e}_1 + c_2u_2\,\mathbf{e}_2)$ (note that $\sigma_\rho(\mathbf{u})$ is independent of the choice of $m_{\max}$ in $\{1,2\}$ since $a_2+c_2 = \pm(a_1+c_1)$). Similar results are obtained by permutation of indices in the cases $|c_1| = |c_3| > |c_2|$ and $|c_2| = |c_3| > |c_1|$. The A-classical states (51) have maximally mixed marginals, although they are not of the form (29) save for $u_1 = 0, \pm 1$ (in fact, $\sigma_\rho(\mathbf{u})$ can be transformed into the state (47) by an appropriate conjugation by a local unitary operator). If $|c_1| = |c_2| = |c_3|$, any orthonormal basis is optimal and one obtains a family of closest states depending on the arbitrary optimal unit vector $\mathbf{u}\in\mathbb{R}^3$, given by (51) with $\mathbf{u}(\mathbf{c}) = c_{m_{\max}}^{-1}(c_1u_1\,\mathbf{e}_1 + c_2u_2\,\mathbf{e}_2 + c_3u_3\,\mathbf{e}_3)$.

Let us now discuss a more subtle point, which is of relevance if one wants to find *all* A-classical states σ_ρ satisfying (44). Given an optimal basis $\{|\alpha_i^{\text{opt}}\rangle\}$, there is not guarantee that the square-root measurement (45) is the only optimal measurement maximizing $P_S(\{\rho_i^{\text{opt}},\eta_i^{\text{opt}}\})$. Actually, it turns out that this is not the case if $\mathbf{c}$ belongs to one of the faces of the tetrahedron (so that $p_0p_1p_2p_3 = 0$). In this situation, we encounter in the appendix a whole family of optimal projectors $\Pi_i^{\text{opt}}(r)$, depending on a real parameter $r\in[-1,1]$. Let us emphasize that if two states of the form (11) with the same optimal basis $\{|\alpha_i^{\text{opt}}\rangle\}$ are the closest A-classical states to ρ then, by convexity of the square Bures distance, any convex combination of these states is also a closest A-classical state to ρ. Hence the set of optimal projectors must be either infinite or reduced to one point. To each measurement in this set one can associate a closest A-classical state by equation (11), which is determined in the appendix. Before giving the result, let us introduce the product basis $\{|\alpha_i,\beta_j\rangle = |\alpha_i\rangle\otimes|\beta_j\rangle\}_{i,j=0}^1$ of

$\mathbb{C}^2 \otimes \mathbb{C}^2$ defined as follows: (i) if $|c_m|$ is maximal for a single index $m = m_{\max}$, then $|\alpha_i\rangle = |\beta_i\rangle$ are the eigenvectors of $\sigma_{m_{\max}}$; (ii) if $|c_m|$ is maximum for exactly two components c_m, then $m_{\max}$, $|\alpha_i\rangle$, and $|\beta_i\rangle$ are defined by

$$m_{\max} = \begin{cases} 1 \\ 3 \\ 3 \end{cases}, \quad |\alpha_i\rangle = \begin{cases} \mathrm{e}^{-\mathrm{i}\frac{\phi}{2}\sigma_3}\frac{|0\rangle+(-1)^i|1\rangle}{\sqrt{2}} & \text{if} \quad c_1 = \pm c_2, |c_1| > |c_3| \\ \mathrm{e}^{-\mathrm{i}\frac{\theta}{2}\sigma_2}|i\rangle & \text{if} \quad c_1 = \pm c_3, |c_1| > |c_2| \\ \mathrm{e}^{\mathrm{i}\frac{\theta}{2}\sigma_1}|i\rangle & \text{if} \quad c_2 = \pm c_3, |c_2| > |c_1| \end{cases}, \tag{52}$$

and

$$|\beta_i\rangle = \begin{cases} \mathrm{e}^{\mp\mathrm{i}\frac{\phi}{2}\sigma_3}\frac{|0\rangle+(-1)^i|1\rangle}{\sqrt{2}} & \text{if} \quad c_1 = \pm c_2, |c_1| > |c_3| \\ \mathrm{e}^{\mp\mathrm{i}\frac{\theta}{2}\sigma_2}|i\rangle & \text{if} \quad c_1 = \pm c_3, |c_1| > |c_2| \\ \mathrm{e}^{\pm\mathrm{i}\frac{\theta}{2}\sigma_1}|i\rangle & \text{if} \quad c_2 = \pm c_3, |c_2| > |c_1| \end{cases} \tag{53}$$

for some arbitrary angles ϕ or $\theta \in [0, 2\pi[$; (iii) if $|c_1| = |c_2| = |c_3|$, that is, $c_1 = \epsilon_2 c_2 = \epsilon_3 c_3$ with $\epsilon_{2,3} \in \{-1, 1\}$, then

$$m_{\max} = 3, \quad |\alpha_i\rangle = \mathrm{e}^{-\mathrm{i}\frac{\phi}{2}\sigma_3}\mathrm{e}^{-\mathrm{i}\frac{\theta}{2}\sigma_2}|i\rangle, \quad |\beta_i\rangle = \mathrm{e}^{-\mathrm{i}\epsilon_2\frac{\phi}{2}\sigma_3}\mathrm{e}^{-\mathrm{i}\epsilon_3\frac{\theta}{2}\sigma_2}|i\rangle \tag{54}$$

for arbitrary angles ϕ and $\theta \in [0, 2\pi[$. Then all the closest A-classical states to ρ are of the following form:

$$\sigma_\rho(r) = \frac{q_{m_{\max}}}{2}\big[|\alpha_0, \beta_0\rangle\langle\alpha_0, \beta_0| + |\alpha_1, \beta_1\rangle\langle\alpha_1, \beta_1|\big] + \frac{1 - q_{m_{\max}}}{2}\big[(1 + r)|\alpha_0, \beta_1\rangle\langle\alpha_0, \beta_1| + (1 - r)|\alpha_1, \beta_0\rangle\langle\alpha_1, \beta_0|\big] \tag{55}$$

if $p_0 p_{m_{\max}} = 0$ and $p_m > 0 \ \ \forall\, m \neq m_{\max}$, and

$$\sigma_\rho(r) = \frac{q_{m_{\max}}}{2}\big[(1 + r)|\alpha_0, \beta_0\rangle\langle\alpha_0, \beta_0| + (1 - r)|\alpha_1, \beta_1\rangle\langle\alpha_1, \beta_1|\big] + \frac{1 - q_{m_{\max}}}{2}\big[|\alpha_0, \beta_1\rangle\langle\alpha_0, \beta_1| + |\alpha_1, \beta_0\rangle\langle\alpha_1, \beta_0|\big] \tag{56}$$

if $p_0 p_{m_{\max}} > 0$ and $p_1 p_2 p_3 = 0$. In these equations $r \in [-1, 1]$ is arbitrary. When $\mathbf{c}$ is in the interior of the tetrahedron $\mathcal{T}$ (i.e., $p_0 p_1 p_2 p_3 > 0$), all the closest states are obtained by setting $r = 0$ in equations (55) and (56). One then recovers the previous results (47) and (51). Therefore, ρ has a unique closest A-classical state if and only if $\mathbf{c}$ is in the interior of $\mathcal{T}$ and the maximum $|\mathbf{c}|$ is non-degenerate (case (i)). In the case (ii), ρ admits a 1-parameter (or, if $\mathbf{c}$ belongs to a face of $\mathcal{T}$, a 2-parameter) family of closest A-classical states. In the case (iii), this family is a 2-parameter (or, if $\mathbf{c}$ belongs to a face of $\mathcal{T}$, a 3-parameter) family.

It should be noted that the states (55) and (56) do not have maximally mixed marginals save for $r = 0$. This means that the states ρ on the faces of $\mathcal{T}$ have closest A-classical states outside the tetrahedron. Let us also emphasize that all the closest A-classical states σ_ρ determined in this section are in fact classical states, that is, the eigenvectors of σ_ρ are product states. Thus

$$D_A(\rho) = D_B(\rho) = 2\left(1 - \sqrt{\frac{1 + b_{\max}}{2}}\right), \tag{57}$$

as could be expected from the symmetry of ρ under the exchange of the two qubits.

In figures 3(*b*) and (*c*), some examples of states ρ in the tetrahedron and their closest states σ_ρ are represented. In figure 3(*b*), outside the dashed lines on which two or more components c_m have equal moduli, σ_ρ is specified by a vector $\mathbf{s}$ lying on the closest coordinate semi-axis to $\mathbf{c}$ for the usual distance in $\mathbb{R}^3$ (but $\mathbf{s}$ is not the closest vector to $\mathbf{c}$ on that semi-axis).

The closest A-classical states for the Hilbert–Schmidt distance d_2 to a state ρ of the form (29) can be found by using the results of [13]. They are given by

$$\sigma_\rho^{(2)}(\mathbf{u}) = \frac{1}{4}\left(1 \otimes 1 + \sum_{l,m=1}^{3} u_l c_m u_m \sigma_l \otimes \sigma_m\right) \tag{58}$$

with an arbitrary unit vector $\mathbf{u} \in \mathbb{R}^3$. In contrast with the Bures distance, all states ρ with maximally mixed marginals have infinitely many closest A-classical states. Moreover, there are three states $\sigma_\rho^{(2)}$ of the form (29) lying on the coordinate axes, with non-vanishing coordinate equal to the corresponding coordinate of $\mathbf{c}$, irrespective of the order of the moduli $|c_m|$. Since $\mathrm{tr}[(\sigma_\rho^{(2)})^2] = (1 + \sum_m c_m^2 u_m^2)/4 \leqslant 1/2$, the closest states $\sigma_\rho^{(2)}$ are always mixed. In particular, unlike for the Bures distance, the closest classical states to the maximally entangled pure states $|\Psi_v\rangle$ are not pure product states.

6. Conclusions

We have shown that the results of [14] can be used to determine the geometric quantum discord (GQD) with Bures distance of a state ρ of a bipartite system AB and the corresponding closest A-classical states to ρ when the subsystem A is a qubit. Analytical expressions for this GQD in the DQC1 model and for two qubits in a state with maximally mixed marginals have been obtained. In all cases for which exact analytical formulas for the usual quantum discord of [4, 5] are also available, we observe that the normalized GQD is smaller than the usual discord. In the DQC1 model, the comparison of the GQDs of the output state for different unitaries U_n shows that the highest discord appears when U_n has uniformly distributed eigenvalues on the unit disk modulo a symmetry with respect to the origin. In particular, the discord cannot be larger than that obtained for large random unitary matrices distributed according to the Haar measure, which have been studied in [7]. For rotation matrices and large number of qubits n, the GQD is close to this upper bound, expected for small rotation angles and at certain specific angles. For two-qubit states ρ with maximally mixed marginals, the closest A-classical states for the Bures distance are qualitatively similar to the closest A-classical states for the relative entropy, but completely different from those for the Hilbert–Schmidt distance. The geometry induced by the Bures distance in the tetrahedron looks like the Euclidean geometry of $\mathbb{R}^3$, the A-classical states being located on the three segments of the coordinate axes inside the tetrahedron. However, depending on the symmetry of ρ, ρ can have either a unique closest classical state with maximally mixed marginals or a continuous family of closest classical states with maximally mixed or non-maximally mixed marginals.

Our results constitute a first step in the study of the geometric measure of quantum discord introduced in [14] in some concrete models and its relation with the usual discord and other geometrical versions. It would be of interest to calculate the Bures-GQD in other physical models, in particular in the presence of dynamical evolutions, and to compare it with other measures of non-classicality in the literature.

Acknowledgments

We acknowledge financial support from the French project no. ANR-09-BLAN-0098-01, the Chilean Fondecyt project no. 100039, and the project Conicyt-PIA anillo no. ACT-1112 'Red de Análisis estocástico y aplicaciones'.

Note added. After the completion of this work we have been informed by G Adesso that the Bures geometric discord for two-qubit states with maximally mixed marginals has been calculated independently in [37] by a different method, yielding to the same result (equation (39)).

Appendix. Closest classical states of a two-qubit state with maximally mixed marginals

In this appendix we determine all optimal projective measurements $\{\Pi_i^{\rm opt}\}$ maximizing the success probability $P_S(\{\rho_i^{\rm opt}, \eta_i^{\rm opt}\})$ in equation (13) for a two-qubit state ρ of the form (29). This allows us to find all the closest A-classical states to ρ by applying formula (11).

Before starting the calculation, let us first note that we can restrict our analysis to optimal directions $\mathbf{u}^{\rm opt}$ satisfying $\mathbf{u}^{\rm opt}\cdot\mathbf{e}_m \geqslant 0$ for a fixed coordinate index $m = 1, 2$, or 3. Indeed, changing the order of the vectors in the basis $\{|\alpha_i^{\rm opt}\rangle\}_{i=0}^1$ in equations (9) and (11) amounts to exchange $(\rho_0^{\rm opt}, \eta_0^{\rm opt}) \leftrightarrow (\rho_1^{\rm opt}, \eta_1^{\rm opt})$ and $\Pi_0^{\rm opt} \leftrightarrow \Pi_1^{\rm opt}$. This does clearly not modify the optimal success probability and the A-classical states σ_ρ. But $\{|\alpha_i^{\rm opt}\rangle\}$ is the eigenbasis of the spin operator $\sigma_{\mathbf{u}}$ for the optimizing direction $\mathbf{u} = \mathbf{u}^{\rm opt}$, see section 3. Changing the order of the basis vectors thus corresponds to invert $\mathbf{u}^{\rm opt}$. Hence we may assume $\mathbf{u}^{\rm opt}\cdot\mathbf{e}_m \geqslant 0$ without loss of generality. Thanks to the results of section 5, we know that if $|c_m|$ is maximal for a single index $m = m_{\max}$ then $\mathbf{u}^{\rm opt} = \mathbf{e}_{m_{\max}}$.

We first study the case $|c_3| > |c_1|, |c_2|$. All other cases will be deduced by symmetry arguments. Then $\mathbf{u}^{\rm opt} = \mathbf{e}_3$ and $|\alpha_i^{\rm opt}\rangle = |i\rangle$ $(i = 0, 1)$ are the vectors of the standard basis. By setting $\theta = 0$ in (34), we immediately find that $\Lambda^{\rm opt} \equiv \Lambda(\mathbf{u}^{\rm opt})$ has eigenvalues $\lambda_+^{\rm opt} = (b_3 + |a_3|)/4 > 0$, $\lambda_-^{\rm opt} = (b_3 - |a_3|)/4 \geqslant 0$, $-\lambda_-^{\rm opt} \leqslant 0$, and $-\lambda_+^{\rm opt} < 0$ (here, we have used the inequalities $b_3 \geqslant |a_3|$ and $b_3 > 0$, which follow from (36)). As stressed in section 3, $\Pi_0^{\rm opt}$ is the projector on the direct sum $\mathcal{V}_+ \oplus \mathcal{V}_-$ of the eigenspaces $\mathcal{V}_+$ and $\mathcal{V}_-$ associated to the maximal eigenvalues $\lambda_+^{\rm opt}$ and $\lambda_-^{\rm opt}$, provided that these eigenvalues are non-degenerated. If $\lambda_-^{\rm opt} = 0$ is two-fold degenerated, any projector on $\mathcal{V}_+ \oplus \mathcal{V}$ with $\mathcal{V} \subset \mathcal{V}_-$ a one-dimensional subspace of $\mathcal{V}_-$ defines an optimal projector $\Pi_0^{\rm opt}$. In view of the diagonal form (34) of $\Lambda^{\rm opt}$ in the standard basis, one gets

$$\Pi_0^{\rm opt} = \begin{cases} |0\rangle\langle 0| \otimes 1 & \text{if} \quad b_3 > |a_3| \\ |00\rangle\langle 00| + |\Phi\rangle\langle\Phi| & \text{if} \quad b_3 = a_3 > 0 \\ |01\rangle\langle 01| + |\Phi'\rangle\langle\Phi'| & \text{if} \quad b_3 = -a_3 > 0 \end{cases} \tag{A.1}$$

with $|\Phi\rangle \in \text{span}\{|10\rangle, |01\rangle\}$ and $|\Phi'\rangle \in \text{span}\{|00\rangle, |11\rangle\}$, $\|\Phi\| = \|\Phi'\| = 1$. The condition $b_3 > |a_3|$ is achieved when all p_ν are nonzero, see (36). Then the optimal measurement $\{\Pi_i^{\rm opt}\}$ is unique and thus ρ has a unique closest A-classical state. The condition $b_3 = a_3$ (respectively $b_3 = -a_3$) corresponds to $p_0 p_3 = 0$ (respectively $p_1 p_2 = 0$), that is, to a vector $\mathbf{c}$ belonging to the faces $F_+F_-G_+$ or $F_+F_-G_-$ (respectively, $G_+G_-F_+$ or $G_+G_-F_-$) of the tetrahedron. In this situation one has infinitely many optimal measurements. Note that $p_0 p_3$ and $p_1 p_2$ cannot both vanish, since otherwise one would have $b_3 = a_3 = 0$, in contradiction with our hypothesis $|c_3| > |c_1|, |c_2|$ (which is equivalent to $b_3 > b_1, b_2 \geqslant 0$ by (41)). Let us replace $|\alpha_i^{\rm opt}\rangle = |i\rangle$ and (A.1) into the expression (11) of σ_ρ and make use of the expression (32) of $\sqrt{\rho}$ in the standard basis. By taking advantage of the identities $t_1 + t_2 = \pm(t_0 - t_3)$ for $p_{0,3} = 0$ and $t_1 - t_2 = \pm(t_0 + t_3)$ for $p_{1,2} = 0$ (which can be established with the help of (33)), a simple lengthy calculation yields

$$\sigma_\rho(r) = \frac{(t_0+t_3)^2}{F_A(\rho)}[|00\rangle\langle 00| + |11\rangle\langle 11|] + \frac{(t_0-t_3)^2}{F_A(\rho)}[(1+r)|01\rangle\langle 01| + (1-r)|10\rangle\langle 10|] \tag{A.2}$$

if $p_0 p_3 = 0$, and

$$\sigma_\rho(r) = \frac{(t_0+t_3)^2}{F_A(\rho)}\big[(1+r)|00\rangle\langle 00| + (1-r)|11\rangle\langle 11|\big] + \frac{(t_0-t_3)^2}{F_A(\rho)}\big[|01\rangle\langle 01| + |10\rangle\langle 10|\big] \tag{A.3}$$

if $p_1 p_2 = 0$. The real parameter r in (A.2) and (A.3) are given by $r = \pm 2\,\mathrm{Re}\{\langle 01|\Phi\rangle\langle\Phi|10\rangle\}$ and $r = \pm 2\,\mathrm{Re}\{\langle 11|\Phi'\rangle\langle\Phi'|00\rangle\}$, respectively. Since $|\Phi\rangle$ and $|\Phi'\rangle$ are arbitrary normalized vectors in the two-dimensional spaces specified after (A.1), r can take any values in $[-1, 1]$. If all p_v are nonzero, the unique closest classical state is given by setting $r = 0$ in (A.2) or (A.3). Recalling that $F_A(\rho) = (1 + b_3)/2 = 4(t_0^2 + t_3^2)$, we find that σ_ρ is given by equations (55), (56), and (50) with $m_{\max} = 3$ and $|\alpha_i\rangle = |\beta_i\rangle = |i\rangle$.

The case $|c_1| > |c_2|, |c_3|$ (respectively $|c_2| > |c_1|, |c_3|$) can be deduced from the previous case by the following symmetry argument. By means of the unitary conjugation $\rho' = U\rho U^\dagger$ with $U = \mathrm{e}^{\mathrm{i}\frac{\pi}{4}\sigma_2} \otimes \mathrm{e}^{\mathrm{i}\frac{\pi}{4}\sigma_2}$ (respectively $U = \mathrm{e}^{-\mathrm{i}\frac{\pi}{4}\sigma_1} \otimes \mathrm{e}^{-\mathrm{i}\frac{\pi}{4}\sigma_1}$), one can transform ρ into a state ρ' of the form (29) with a vector $\mathbf{c}' = (c_3, c_2, c_1)$ (respectively $\mathbf{c}' = (c_1, c_3, c_2)$) satisfying $|c_3'| > |c_1'|, |c_2'|$. By invariance of the fidelity (6) and of $\mathcal{C}_A$ under local unitary conjugations, such a transformation does not change F_A, so that $F_A(\rho) = F_A(\rho') = (1 + b_3')/2 = (1 + b_{\max})/2$, in agreement with (39). Moreover, according to (44), the states σ_ρ are related to the closest states $\sigma_{\rho'}$ to ρ' by $\sigma_\rho = U^\dagger \sigma_{\rho'} U$. But $\sigma_{\rho'}$ is given by (A.2) and (A.3) upon the replacement of t_3 by $t_3' = t_{\max}$. Therefore, σ_ρ is given by equations (55) and (56) in which $|\alpha_i\rangle = |\beta_i\rangle$ are the eigenvectors of $\sigma_{m_{\max}}$ with eigenvalues $(-1)^i$, that is, $|\alpha_i\rangle = \mathrm{e}^{-\mathrm{i}\frac{\pi}{4}\sigma_2}|i\rangle \propto |0\rangle + (-1)^i|1\rangle$ if $|c_1| > |c_2|, |c_3|$ and $|\alpha_i\rangle = \mathrm{e}^{\mathrm{i}\frac{\pi}{4}\sigma_1}|i\rangle \propto |0\rangle + \mathrm{i}(-1)^i|1\rangle$ if $|c_2| > |c_1|, |c_3|$.

We now turn to states ρ with vectors $\mathbf{c}$ such that $|c_m|$ is maximum for exactly two components c_m. For instance, let us assume $c_1 = \pm c_2$ and $|c_1| = |c_2| > |c_3|$ (the other cases will easily follow by a state rotation as above). Then, as noted in section 5.3, any vector $\mathbf{u}_\phi = \cos\phi\,\mathbf{e}_1 + \sin\phi\,\mathbf{e}_2$ in the (xOy)-plane defines an optimal direction. The corresponding optimal basis is formed by the eigenvectors $|\alpha_{\phi,i}^{\mathrm{opt}}\rangle = \mathrm{e}^{-\mathrm{i}\frac{\phi}{2}\sigma_3}|\alpha_{0,i}^{\mathrm{opt}}\rangle$ of $\sigma_{\mathbf{u}_\phi}$ with eigenvalues $(-1)^i$. The non-uniqueness of $\mathbf{u}^{\mathrm{opt}}$ comes from the symmetry of ρ. Actually, one finds from (29) that for any angle $\phi \in [0, 2\pi[$,

$$\rho = U_\pm(\phi)\rho\,U_\pm(-\phi), \quad U_\pm(\phi) = \mathrm{e}^{-\mathrm{i}\frac{\phi}{2}\sigma_3} \otimes \mathrm{e}^{\mp\mathrm{i}\frac{\phi}{2}\sigma_3}. \tag{A.4}$$

By using (15) and the identity $\mathrm{e}^{\mathrm{i}\frac{\phi}{2}\sigma_3}\sigma_{\mathbf{u}}\,\mathrm{e}^{-\mathrm{i}\frac{\phi}{2}\sigma_3} = \sigma_{\mathbf{u}'}$, where $\mathbf{u}'$ is related to $\mathbf{u}$ by a rotation around the z-axis with the angle $-\phi$, it follows that

$$\Lambda(\mathbf{u}_\phi) = U_\pm(\phi)\Lambda(\mathbf{e}_1)U_\pm(-\phi). \tag{A.5}$$

As a result, the spectral projectors $\Pi_{\phi,i}^{\mathrm{opt}}$ of $\Lambda(\mathbf{u}_\phi)$ and thus the closest classical state (11) corresponding to $\mathbf{u}^{\mathrm{opt}} = \mathbf{u}_\phi$ are obtained from the corresponding projectors and classical state for $\mathbf{u}^{\mathrm{opt}} = \mathbf{e}_1$ by a unitary conjugation by $U_\pm(\phi)$. But the closest classical state for $\mathbf{u}^{\mathrm{opt}} = \mathbf{e}_1$ is given by (A.2) and (A.3) upon the substitution of t_3 by t_1 and of $|0\rangle, |1\rangle$ by the eigenvectors of σ_1. We conclude that the states σ_ρ are given by (55) and (56) with $m_{\max} = 1$ and the vectors $|\alpha_i\rangle$ and $|\beta_i\rangle$ as in equation (52).

Finally, let us study the states ρ with $|c_1| = |c_2| = |c_3|$. This is the case for instance for the Werner states. Let $\epsilon_2, \epsilon_3 \in \{-1, 1\}$ be defined by $c_1 = \epsilon_2 c_2 = \epsilon_3 c_3$. Then ρ is invariant under rotations with arbitrary angles θ and ϕ,

$$\rho = U_{\epsilon_2,\epsilon_3}(\theta,\phi)\rho\,U_{\epsilon_2,\epsilon_3}(\theta,\phi)^\dagger, \quad U_{\epsilon_2,\epsilon_3}(\theta,\phi) = \mathrm{e}^{-\mathrm{i}\frac{\phi}{2}\sigma_3}\mathrm{e}^{-\mathrm{i}\frac{\theta}{2}\sigma_2} \otimes \mathrm{e}^{-\mathrm{i}\epsilon_2\frac{\phi}{2}\sigma_3}\mathrm{e}^{-\mathrm{i}\epsilon_3\frac{\theta}{2}\sigma_2}. \tag{A.6}$$

Moreover, the eigenvalues of $\Lambda(\mathbf{u})$ are independent of $\mathbf{u}$, since $b_1 = b_2 = b_3$, see (37) and (41). Thus the optimal direction $\mathbf{u}^{\mathrm{opt}}$ is completely arbitrary and any orthonormal basis $\{|\alpha_i^{\mathrm{opt}}\rangle\}$ of $\mathbb{C}^2$ is optimal. The closest classical states to ρ are again given by (55) and (56), with the vectors $|\alpha_i\rangle$ and $|\beta_i\rangle$ as in equation (54).

References

[1] Nielsen N A and Chuang I L 2000 *Quantum Computation and Information* (Cambridge: Cambridge University Press)

[2] Horodecki R, Horodecki P, Horodecki M and Horodecki K 2009 *Rev. Mod. Phys.* **81** 865
[3] Modi K, Brodutch A, Cable H, Paterek T and Vedral V 2012 *Rev. Mod. Phys.* **84** 1655
[4] Ollivier H and Zurek W H 2001 *Phys. Rev. Lett.* **88** 017901
[5] Henderson L and Vedral V 2001 *J. Phys. A: Math. Gen.* **34** 6899
[6] Bennett C H, DiVincenzo D P, Smolin J A and Wootters W K 1996 *Phys. Rev.* A **54** 3824
[7] Datta A, Shaji A and Caves C M 2008 *Phys. Rev. Lett.* **100** 050502
[8] Lanyon B P, Barbieri M, Almeida M P and White A G 2008 *Phys. Rev. Lett.* **101** 200501
[9] Passante G, Moussa O, Trottier D A and Laflamme R 2011 *Phys. Rev.* A **84** 044302
[10] Fanchini F F, Cornelio M F, de Oliveira M C and Caldeira A O 2011 *Phys. Rev.* A **84** 012313
[11] Knill E and Laflamme R 1998 *Phys. Rev. Lett.* **81** 5672
[12] Datta A, Flammia S T and Caves C M 2005 *Phys. Rev.* A **72** 042316
[13] Dakić B, Vedral V and Brukner C 2010 *Phys. Rev. Lett.* **105** 190502
[14] Spehner D and Orszag M 2013 *New J. Phys.* **15** 103001
[15] Wei T C and Goldbart P M 2003 *Phys. Rev.* A **68** 042307
[16] Streltsov A, Kampermann H and Bruß D 2010 *New. J. Phys.* **12** 123004
[17] Maziero J, Céleri L C, Serra R M and Vedral V 2009 *Phys. Rev.* A **80** 044102
[18] Mazzola L, Piilo J and Maniscalco S 2010 *Phys. Rev. Lett.* **104** 200401
[19] Helstrom C W 1976 *Quantum Detection and Estimation Theory* (New York: Academic)
[20] Bergou J A, Herzog U and Hillery M 2004 Discrimination of quantum states in *Quantum State Estimation* (*Lecture Notes in Physics* vol 649) ed M Paris and J Rehacek (Berlin: Springer) pp 417–65
[21] Eldar Y C 2003 *Phys. Rev.* A **68** 052303
[22] Uhlmann A 1976 *Rep. Math. Phys.* **9** 273
[23] Bures D 1969 *Trans. Am. Math. Soc.* **135** 199
[24] Petz D 1996 *Linear Algebra Appl.* **244** 81
[25] Braunstein S L and Caves C M 1994 *Phys. Rev. Lett.* **72** 3439
[26] Eldar Y C, Megretski A and Verghese G C 2004 *IEEE Trans. Inform. Theory* **50** 1198
[27] Chou C-L and Hsu L Y 2003 *Phys. Rev.* A **68** 042305
[28] Qiu D and Li L 2010 *Phys. Rev.* A **81** 042329
[29] Helstrom C W 1982 *IEEE Trans. Inform. Theory* **28** 359
[30] Jezek M, Rehácek J and Fiurásek J 2002 (arXiv:0201108 [quant-ph])
[31] Bhatia R 1996 *Matrix Analysis* (*Graduate texts in Mathematics* vol 169) (Berlin: Springer)
[32] Horodecki R and Horodecki M 1996 *Phys. Rev.* A **54** 1838
[33] Luo S 2008 *Phys. Rev.* A **77** 042303
[34] Modi K, Paterek T, Son W, Vedral V and Williamson M 2010 *Phys. Rev. Lett.* **104** 080501
[35] Wootters W K 1998 *Phys. Rev. Lett.* **80** 2245
[36] Girolami D and Adesso G 2011 *Phys. Rev.* A **83** 052108
[37] Aaronson B, Franco R L and Adesso G 2013 *Phys. Rev.* A **88** 012120